Bio-inspired self-prestressing concrete (SPC) involving basalt fibers and expansive agent

S.H. Chu[1,2,*], M. Khan[1], X.W. Deng[1], C. Unluer[3]

[1] Department of Civil Engineering, The University of Hong Kong, Hong Kong, China
[2] School of Civil and Environmental Engineering, Nanyang Technological University, Singapore
[3] School of Engineering, University of Glasgow, Glasgow G12 8LT, United Kingdom

Abstract:

Inspired by muscle structure, the synergy between basalt fibers (BF) and expansive agent (EA) was revealed and utilized for the development of self-prestressing concrete (SPC). When BF and EA were used together, the restraining action of BF against the autogenous expansion of concrete yielded active confining stress, during which fibers were prestressed, producing SPC. The properties of SPC were investigated by varying BF (0-0.6%) and EA (0-3%) contents. The addition of EA and/or BF decreased workability but improved mechanical performance. The strength-workability envelopes revealed the superiority of the combined use of EA and BF, whose synergistic effect was analysed both qualitatively and quantitatively. Possible mechanisms behind their contribution to sample performance was discussed considering passive and active confinements. Scanning electron microscopy images revealed improvement in the fiber-matrix interface with an increase in the amount of EA. This bio-inspired work shall be beneficial to the development of SPC with improved performance.

Keywords: Composite (E); compressive strength (C); expansion (C); fiber reinforcement (E).

[*] Corresponding author. Email: shchu@connect.hku.hk (S.H. Chu)

1. Introduction

Fiber reinforced concrete (FRC), including strain-hardening cementitious composite (SHCC), has been prevalent as it conquers the intrinsic brittleness and low tensile performance of conventional concrete [1,2]. Fibers are indispensable components in the development of FRC/SHCC to acquire higher performance [3]. When under compression, regular concrete (i.e. without the use of fibers) could dilate and crack, thus accelerating its rapid deterioration and causing brittle failure [4,5]. The addition of fibers could restrain the dilation and delay the crack propagation, owing to its confinement effect [6]. Alternatively, when under tension, concrete could suddenly crack, which could be alleviated via the addition of fibers that could increase the first cracking strength and create a higher post cracking strength. This mechanism, referred to as strain-hardening behavior, during which multiple-cracking phenomena could appear, is accompanied by larger energy absorption capacity [7-9]. Above all, the addition of fibers could substantially improve concrete performance due to its confining effect and bridging effect.

Among the various types of fibers, both organic fibers (e.g. polyvinyl alcohol (PVA) fibers) [10,11] and inorganic metallic fibers (e.g. steel fibers) are widely used for improving the ductility and strength [12,13]. Previous studies [14,15] reported that strain-hardening behavior of FRC could generally be achieved using 2% PVA fibers by volume. Similarly, the positive effects of the addition of 2% steel fibers on compressive strength, tensile strength and rebar bond strength of FRC mixes were also revealed [16-18]. Despite the substantial effectiveness of fibers in enhancing the performance of concrete, both types of fibers are associated with durability concerns, with organic fibers being vulnerable to aging and fire, whereas inorganic metallic fibers are susceptible to corrosion [19-21]. Therefore, there is a need to develop materials with improved durability to resist self-deterioration and environmental attacks and provide adequate strength to enable a strong composite material.

Inorganic non-metallic fibers, such as basalt fibers (BF) and carbon fibers have been gaining increased attention in the literature [22,23]. BF, due to its relatively lower cost and high compatibility with concrete mixtures, has been investigated in several studies [24-27]. The use of up to 7.5% BF in hybrid FRC led to up to 16% increase in flexural strength [26]. Another study [27] that incorporated up to 0.2% BF in concrete revealed an increase in 28-day compressive strength from 96.5 to 103.4 MPa and flexural strength from 8.3 to 9.6 MPa. This improvement in mechanical performance in the presence of BF was associated with delayed formation and propagation of microcracks.

Another approach for improving concrete performance involves the addition of expansive agent (EA) into the mix design [28-30]. Based on the formation of ettringite, EA can be classified into K-, S- and M-types, in accordance with ACI standard [31]. So far, controversy continues on the full understanding of the

expansion mechanism. Prevalent hypotheses in the literature are: (i) crystallization pressure by anisotropic crystals growth [32]; (ii) absorption of water by colloidal ettringite [33]; (iii) hydration of an anhydrous phase to form multi-hydrated phases [33]; and (iv) formation of coexisting pores by disintegration of expansive ingredients during hydration/osmotic pressure [34]. Nevertheless, it is generally accepted that an expansion is incurred by the formation of ettringite when the matrix reaches a certain degree of rigidity. Regarding the application, EA has been used to counterpart shrinkage and reduce the risk of cracking induced by drying shrinkage, particularly in massive concrete used in the construction of dams and foundations of high-rise buildings [35-38]. The use of EA was revealed to result in a higher bond strength and better tension-stiffness performance due to the chemical prestressing effect [39]. Another use for expansive concrete was suggested in the constrained region of reinforced concrete structures to act in a way similar to prestressed concrete structure [40]. Further studies [41] reported that the improved mechanical strength and ductility of concrete beams made with expansive concrete, carbon fiber reinforced polymer sheets and steel bars. However, at the material level, the inner microstructure of expansive cement paste and concrete subjected to free-curing conditions was revealed to be loose, with many cracks in the paste and paste-aggregate interface. Alternatively, a confined-curing condition could improve the microstructure of expansive concrete by intensifying and densifying the paste-aggregate interface [42]. Considering that confined-curing conditions may not always be available or feasible, particularly for in-situ construction [43, 44], it is imperative to solve this problem by providing sufficient confinement to better utilize the beneficial effects of EA.

Inspired by muscle structure, an innovative and promising way to solve the above problem is the combined use of BF and EA. While the individual use of BF and EA has been widely reported in literature, their combined use and the possible synergistic effect between BF and EA has not been fully explored. A chemical prestress could be developed along the fibers when the autogenous expansion induced by chemical reactions of the EA was restrained by the fibers in the matrix. On the other hand, when the volume of concrete is confined, the autogenous expansion could give rise to a stress perpendicular to the length of fiber and such stress surrounding fibers could improve the bond at the fiber-matrix interface [42-44]. Such confining effect arising from the use of EA has been evidenced by a recent study [30], where the use of EA in lightweight aggregate concrete increased the confinement effectiveness by 83%, which translated into 23% increase in the confined strength when a rigid formwork was used as temporary confinement. Previous studies [43] exploring the addition of hybrid steel, polypropylene and polyvinyl alcohol fibers and EA reported an improvement in the shrinkage and permeability resistance of high-performance concrete mixes at the combined use of hybrid fiber and EA. However, no synergistic effect between fibers and EA were identified. Another study [35] reported the beneficial effect of the combined use of brass-coated steel fibers and CaO-based EA on flexural strength, which was attributed to the improved fiber-matrix interface due to formation of calcium-hydroxy-zincate crystals.

Based on these previous findings on the improvement of the bond at the fiber-matrix interface in the presence of various fibers and EA, this paper focuses on the development of bio-inspired self-prestressing concrete (SPC) incorporating the simultaneous use of BF and EA to enhance performance. Biologically, appropriate exercise could boost the formation of sturdy muscles that can withstand greater forces via the strengthening and prestressing of the muscle fiber by the surrounding tissues and blood pressure, particularly when activated [45-49]. Inspired by this mechanism, this study aims to develop SPC incorporating the combined use of BF and EA, whose synergistic effect in cement-based mixes has not been fully explored until now. To fill this gap in the literature, a detailed experimental program was designed to reveal the potential individual and synergistic effect of various amounts of BF and EA on the fresh and hardened properties of mortar mixes.

2. Materials and Methodology

2.1 Materials

CEM I ordinary Portland cement (OPC) of class 52.5R, in accordance with BS EN 197-1, was used. To produce mortar mixtures, quartz sand (QS) with a maximum size of 1.18 mm was adopted. BF (length =12 mm, aspect ratio = 923, specific gravity = 2.60, tensile strength = 1225 MPa and Young's modulus = 60 GPa), as shown in Fig. 1(a), was used. The EA, as shown in Fig. 1(b), consisted mainly of calcium aluminate, calcium sulphate, aluminium oxide, magnesium oxide and calcium oxide, complying with Chinese Standard GB 23439-2017 [50]. Table 1 shows the properties of EA. The expansion effect of the EA used was associated with the formation of ettringite. The specific gravities of OPC and EA were determined as 3.11 and 2.87, respectively.

2.2 Mixture design

A total of 16 mortar mixtures containing different BF volume (V_{BF}) and EA content, were prepared. The V_{BF} was varied from 0%, 0.2%, 0.4% to 0.6% with respect to the total volume of the mixture. The EA content varied from 0%, 1%, 2% to 3% in replacement of the paste volume. To exclude the effect of QS, the volume of QS was kept constant at 25% of the total volume of all mixtures. The water to cement (W/C) ratio was fixed at 0.55. Table 2 presents the detailed mixture proportions for one cubic meter of the mixture. Each mortar mixture was labelled in the form of X-Y-Z, in which X denoted the W/C ratio, Y denoted the EA volume (%) and Z denoted the V_{BF} (%).

2.3 Workability test

The workability of the mortar mixtures was determined by a mini-slump cone [51, 52], whereby the height reduction of the mortar mix after the lift-up of the slump cone was measured as the slump. Four perpendicular diameters of the mortar patty were averaged to calculate the flow diameter for each mix. Sieve segregation test was conducted using a sieve size of 1.18 mm to analyze the cohesiveness. The mass ratio of mortar that was dipped through the sieve to mortar that was poured onto the sieve was recorded as sieve segregation index (SSI) [10]. Accordingly, the larger the SSI value, the easier it was for the to be mortar separated from the patty, which translated into a lower cohesiveness.

2.4 Specimen preparation

Immediately after the workability tests, the mixture was re-mixed and cast into three carbon steel cubic molds with dimensions of 40×40×40 mm and three carbon steel prismatic molds with dimensions of 40×40×160 mm for compressive strength and flexural tests, respectively. All samples were cured in a water tank set at a temperature of 27±3°C for 28 days [53].

2.5 Compressive strength test

The compression tests were conducted on cube specimens by using a machine with a capacity of 3000 kN, in accordance with BS EN 12390-3:2019 [54]. During the compression tests, the loading rate was kept at 3 kN/s for all specimens. Compressive strength results of each mix were averaged from three specimens cast from the same batch and tested on the same day.

2.6 Flexural strength test

Three-point bending tests were performed on prism specimens by using a computer-controlled machine with a capacity 50 kN, in accordance with BS EN 12390-5:2019 [55]. Displacement control was adopted at a loading rate of 0.6 mm/min for all specimens. To avoid uneven stress distribution, the molded surfaces were selected as the load bearing surface. For each mix, three test results were averaged for the final result.

2.7 Scanning electron microscopy (SEM) analysis

To investigate the effect of the addition of increasing the amount of EA on the fiber-matrix interface, a Hitachi S–3400 N scanning electron microscope was employed. To prepare the samples for SEM analysis, the selected mortar samples were sliced and impregnated with epoxy. They were then placed into a vacuum container and cured for 3 days before being ground to 1 μm in preparation for SEM.

3. Results

3.1 Workability

The workability results of all mixes are reported in Table 3, whereas the variation of slump under different BF and EA contents is shown in Fig. 2. The results revealed that at a given EA content, the slump slightly decreased with an increase in V_{BF}. A similar relationship between slump and EA content was observed, where the slump decreased with increasing EA content. The slump loss due to the incorporation of BF was associated with the intensifying fiber entanglements that lowered the flowability of the mixture. Alternatively, the slump loss due to the addition of EA was caused by the increased amount of water consumption. The chemical reaction of EA with water could consume water and lower down the workability. Fig. 3 depicts the variation of flow diameter with V_{BF} at various EA contents. Similar to the trend observed in slump measurements, the physical effect of BF and the chemical effect of EA concurrently led to lower flow diameters. Nevertheless, the degree of levelling calculated from the slump and flow diameters varied in the narrow range of 0.515-0.586, indicating that the dispersion of BF was acceptable and the prepared mixtures did not suffer obvious segregation from fiber agglomeration.

3.2 SSI

Fig. 4 illustrates the relationship between SSI and different BF and EA contents. Differing from the trend observed in slump and flow diameter measurements, peak points occurred in SSI curves as the V_{BF} increased from 0% to 0.2%, beyond which the SSI decreased again. This trend was more obvious at lower EA contents. The initial increase in SSI at a V_{BF} content of up to 0.2% was due to the decrease in the cohesiveness of the mortar mixture with the addition of fibers. This change could be associated with the densification of the packing of different constituents forming the mix and the increased amount of excess water that could facilitate the movement of particles [56]. As the V_{BF} further increased, the SSI decreased due to the increased resistance to the separation of the paste from the mortar mixture provided by the fibers.

3.3 Compressive strength

The compressive strength results, each averaged from the results of three specimens, together with corresponding standard deviations (S.D.) were reported in Table 4. The relationship between different BF and EA contents is also shown in Fig. 5. Generally, the addition of BF has a positive effect on strength, as evidenced by the increasing trend of compressive strength with higher V_{BF}, which was associated with the confining effect of BF [20]. Alternatively, the incorporation of EA contributed to the strength development by enhancing the formation of hydration products [57]. When the effect of the addition of 0.6% BF vs. 3% EA on strength were compared, the latter has a higher influence in strength enhancement. Moreover, when BF and EA were concurrently used, the compressive strength was elevated to a value much higher than that of the sole addition of each component. Mixes containing 0.6% BF and 3% EA revealed the highest compressive strength of 43.3 MPa, which was ~19% higher than the mixes in which they were omitted or individually used (e.g. 36.4-37.5 MPa)

As an increase in the EA content was reflected as a decrease in the cement content, the relationship between compressive strength and the cement content was illustrated in Fig. 6. At a constant W/C ratio, the compressive strength decreased with the cement content, which was more pronounced at higher BF contents. This was attributed to the decreased amount of EA as paste replacement and intensifying BF bridging effect. Out of all the mixes, those containing 0.6% BF revealed the highest compressive strengths when the cement content was minimum, whereas the QS content was kept constant for all mixes.

Considering that the cement content changed with the addition of EA, the changes in the strength/cement ratio (i.e. the compressive strength divided by the volumetric ratio of cement in the mixture) with respect to V_{BF} is shown in Fig. 7. Generally, an increase in the strength/cement ratio was observed with the BF and EA contents, whilst the highest strength/cement ratio was revealed by the mixtures involving the combined use of BF and EA. The increase in strength with the increase in the BF and EA contents demonstrated the higher contribution of the binder to mechanical performance in the presence of these components.

3.4 Flexural strength

The flexural strength of each prism specimen was calculated by using Equation 1, where f_f is the flexural strength, F is the maximum bending load, L is the span, and b and d are the width and depth of the prism specimen, respectively.

$$f_f = \frac{3FL}{2bd^2} \quad (1)$$

Based on the tests results in Table 4, and the relationship between the flexural strength and V_{BF} shown in Fig. 8, an increase in strength was observed with the addition of BF and EA. A clear trend elucidating the beneficial effects of the increasing contents of BF and EA on the flexural strength was revealed. Differing from the trend observed in the compressive strength, the inclusion of BF seemed to have a similar effect on the increase in flexural strength than the addition of EA. More importantly, the combined use of BF and EA gave rise to the largest increase in flexural strength, revealing the highest flexural strength of 8.68 MPa amongst all samples. This level of strength could not be achieved with the single use of either BF or EA under the prescribed experimental conditions, implying the synergy between these components in enhancing the mechanical performance.

Cement consumption was lowered and the paste volume was kept the same when EA was incorporated into the prepared mixes as cement replacement. Therefore, it is also necessary to evaluate the effectiveness of equal volume of cement in flexural strength enhancement. Accordingly, the flexural strength was plotted against the cement content for mixes containing different V_{BF} in Fig. 9; while the flexural strength/cement ratio was plotted against V_{BF} for mixes containing different EA contents in Fig. 10. A higher flexural strength was achieved at lower cement contents when EA was adopted as paste replacement (Fig. 9). The incorporation of higher amounts of BF further elevated the flexural strength, proving that the combined use of BF and EA could simultaneously facilitate the strength development, meanwhile reducing the cement content. Increases in both the BF and EA contents led to a higher flexural strength/cement ratio (Fig. 10). The highest strength/cement ratio occurred in the combined presence of 0.6% BF and 3.0% EA, demonstrating the benefits of both components in enhancing the efficiency of the binder in terms of its mechanical performance.

4. Discussion on the synergistic effect of BF and EA

4.1 Synergistic effect of BF and EA on compressive strength

Since the addition of BF and EA yielded different positive effects on the compressive strength at different combinations, there is a need to figure out the individual effect of adding BF at given EA contents, the individual effect of adding EA at given BF contents and the combined effect of adding both BF and EA on compressive strength. In this regard, the percentage increases in compressive strength due to the inclusion of BF and/or EA are reported in the second column of Table 5. The compressive strength benefited from the increased incorporation of BF and EA. For instance, at the EA content of 1.0%, the addition of BF at V_{BF} of 0.2%, 0.4% and 0.6% led to 2.5%, 2.0% and 0.2% increases in compressive strength; whereas, at the EA content of 3.0%, the addition of BF at V_{BF} of 0.2%, 0.4% and 0.6% led to 4.8%, 9.3% and 15.6% increases

in compressive strength. These findings highlighted the effectiveness of BF in enhancing mechanical performance in the presence of increasing EA contents. A similar outcome was observed regarding the use of EA in the presence of increasing BF content, resulting in a strength increase of up to 18.9% in mixes containing 3% EA and 0.6% BF, which indicated the effectiveness of EA in contributing to performance in the presence of increasing BF contents. Overall, it can be inferred from the above observations that the effectiveness of the use of BF or EA in strength enhancement would be more remarkable in the presence of the other.

For easier comparison, the percentage increases in compressive strength due to the addition of both BF and EA at various contents in comparison to the strength of plain mixture without the addition of them are tabulated in the second column of Table 5. It revealed that the combined use of BF and EA yielded larger percentage increases in compressive strength than the sum of the percentage increases brought by the corresponding sole addition of BF and EA. For instance, for the mixture containing 3% EA and 0.6% BF, the compressive strength was 19.1% higher than that of the plain mixture and value of 19.1% was much larger than the sum of percentage increase of 0.2% induced by the addition of 0.6% BF at 0% EA and percentage increase of 3.0% induced by the addition of 3% EA at 0.0% BF.

Apparently, the spillover value of 19.1% - (0.2% + 3.0%) = 15.9% demonstrated the synergistic effect of BF and EA on the compressive strength. The extra percentage increases in compressive strength arising from the combined use of BF and EA after deducting the percentage increases brought by the individual use of BF and EA respectively were defined as synergistic effect [24]. The values for all the mixtures with both BF and EA are reported the last column of Table 6. Overall, for the mixtures containing EA not less than 2% and BF not less than 0.4%, the values of synergistic effect were larger than 5.0% and as large as 15.9% which could hardly be deemed as insignificant. Utilizing such synergistic effect between BF and EA, SPC could be developed and the behind mechanism would be presented in the next section.

4.2 Synergistic effect of BF and EA on flexural strength

A similar methodology as the above was adopted to analyze the effect of adding BF/EA at given EA/BF contents on the flexural strength of SPC. The percentage increases in flexural strength are reported in the last column of the Table 5. From the table, the addition of BF generally led to larger percentage increases in flexural strength at a larger EA content. For instance, percentage increases of 8.5%, 10.8%, 10.2% and 13.1% in flexural strength could be achieved by adding 0.4% BF at the EA contents of 0%, 1%, 2% and 3%, respectively. Moreover, at increasing BF contents, the percentage increases became larger, implying there also exist certain synergistic effect between BF and EA on the flexural strength. In addition, at a given BF content,

the incorporation of increasing amounts of EA would generally give rise to larger percentage increases in flexural strength. These phenomena suggested that the effectiveness of BF/EA in enhancing the flexural strength was generally more conspicuous in the presence of larger amounts of EA/BF.

Subsequently, the combined addition of BF and EA would lead to larger percentage increases in flexural strength with respect to the flexural strength of the mixtures without the addition of BF and EA. These percentage increases are tabulated in the second column of the Table 7. Noticeably, the simultaneous addition of 2% EA and 0.4% BF enhanced the flexural strength by 17.3% which was a value greater than the sum of percentage increase of 6.4% due to the addition of 2% EA at 0.0% BF and the percentage increase of 8.5% due to the addition of 0.4% BF at 0% EA. Such quantitative expressions of the synergistic effect on flexural strength were calculated to be positive values (4.8-13.4%) for all the SPC mixtures, demonstrating beneficial effect on flexural strength of SPC by utilizing both BF and EA.

5. Discussion on the strength-workability relation and influencing mechanisms

5.1 Strength-workability relation

As the addition of BF or EA decreased the workability while increase the compressive strength and flexural strength from the section 4, it is not easy to directly evaluate the beneficial effect of using BF (added in terms of the total volume of the mixture) and EA (added as paste replacement). To conquer such difficulties, the envelopes of compressive strength and flexural strength against slump and flow diameter are depicted in Fig. 11 and Fig 12, respectively, to evaluate the concurrent strength-workability performance. In fact, concurrent high strength and workability is not easy to achieve for mixtures with varying BF and EA contents, especially when W/C ratio and superplasticizer dosage were fixed.

Fig. 11 illustrates that, at the same slump or flow diameter, the compressive strengths were generally larger at increasing BF content. Even though the addition of BF or EA decreased the workability, mixtures exhibiting the superior concurrent strength-workability performance were mixtures containing both BF and EA. In addition, the highest compressive strength occurred to the mixture containing 0.6% BF and 3% EA with acceptable slump and flow diameter of 43 mm and 211 mm, respectively. Fig. 12 revealed that, at a given slump or diameter, a higher flexural strength could be achieved after the addition of increasing BF contents. Despite that both BF and EA have negative effect on workability, the optimum concurrent flexural strength-workability performance mostly occurred to the mixtures containing both BF and EA. The mixture containing 0.6% BF and 3% EA exhibited the highest flexural strength.

Fig. 11 and Fig. 12 clearly show that, by varying the contents of BF and EA, the envelope of concurrent strength-workability performance can be pushed towards upper-left for improved strength whilst maintaining acceptable workability for overall enhanced performance. The influences of the addition of EA on workability became more noticeable when it was added as paste replacement because the total water to powder content ratio has been increased. However, such impaired workability could be compensated by adding a suitable amount of superplasticizer. It is only that, in the present study, this common practice has not been adopted to render the mixture comparable and better guarantee the consistency.

5.2 Parallel analysis utilizing existing data

Previous studies on the concurrent use of BF and EA are rather limited to the best knowledge of the authors. Nevertheless, relevant studies were summarized for parallel analysis. In 2001, Sun et al. [43] reported the shrinkage and permeability results of a series of cement-based mixtures (water to binder ratio was fixed at 0.32) and observed that for plain concrete without fibers, the relative permeation coefficient was decreased from 2.9×10^{-7} to 1.7×10^{-7} cm/h when 12% expansive agent (by mass of binder) was included; while at steel fiber (diameter: 0.43 mm; length: 25 mm) volume of 1.5%, the relative permeation coefficient was decreased from 2.0×10^{-7} to 1.0×10^{-7} cm/h when 12% expansive agent (by mass of binder) was included, implying that the permeability was decreased at the combined addition of steel fibers and expansive agent. The enhancement in impermeability shall be closely associated with self-prestressing mechanism. Unfortunately, the compressive strength results have not reported in this interesting work [43]. In 2011, Wang et al. [58] prepared 4 concrete mixes (W/C ratio = 0.42) with the addition of either steel fibers or MgO-based expansive agent or both of them, including one control mix without the addition of them, and found that the 28-day compressive strength changed from 57.5 MPa (estimated from the figure for the control concrete mix), 56.6 MPa (estimated from the figure), 64.9 MPa (estimated from the figure), to 67.6 MPa (estimated from the figure) when 27.2 kg/m^3 MgO-based expansive agent was added, 78 kg/m^3 was added and both of them were added to the control concrete mix. Despite the limited number of mixes and limited data (the number of specimens for each mix and the standard deviation were not reported), it can be roughly referred that the combined addition of steel fibers and expansive agent presented certain synergistic effect that has not been further explored and quantified. In addition, some speculations from the perspective of reduced pore volume and pore size measured by mercury intrusion porosimetry and improved bond at the fiber-matrix interface were given for explaining the observed phenomena [58]. These preliminary experimental results echoed the systematic investigations and findings in the present work. However, the mechanism behind the synergistic effect of fibers and expansive agent has not been systemically elaborated.

5.3 Mechanisms behind the synergistic effect of BF and EA

Chemically, the expansion effect herein mainly arised from the formation of ettringite ($3CaO{\cdot}Al_2O_3{\cdot}3CaSO_4{\cdot}32H_2O$) by virtue of the expansive components mixed in the fresh mixture [59]. After setting, the volume of the hardening paste increased to create an expansion. Depending on its magnitude, the expansion was either used to compensate for volume decrease due to shrinkage or induce tensile stress in reinforcement, as outlined in ACI 223R-10 [31]. Although determining the mechanism responsible for expansion is still a controversial issue today, the materials used are the same as those used to produce OPC concrete, apart from EA [31]. Therefore, tailoring the composition and dosage of EA [32] is necessary for controlling when and how expansion occurs in the matrix. For instance, Bizzozero et al. [32] found a critical amount of gypsum (~45 mol% for calcium aluminate cement and ~55 mol% for sulfoaluminate cement systems) that led to unstable expansion. Herein, the amount of EA was determined based on previous studies [6], which was demonstrated to be effective. Nevertheless, the controlling mechanism for achieving tailorable expansion and the relationship between porosity and expansion are worthy of further systematic exploration [60].

In light of the above experimental investigations and chemical reactions, the possible mechanisms behind the synergistic effect of BF and EA are worthy of further exploration. The beneficial effect of BF and EA on strength development was attributed to the following reasons: first, an expansion occurred to concrete as a result of the incorporation of suitable amount of EA and the expansion would be restrained by the provision of BF [61]; then, stresses along the BF was generated due to the restraining forces, thus prestressing each BF during hardening process of the fiber composites based on which SPC was developed; third, when the SPC was confined within a certain volume during hardening process, the confinement against expansion of concrete could yield compressive stress in the concrete, and compressive stress could then transfer to the fiber-mixture interface at which the bond between them was further enhanced; lastly, the combined mechanisms simultaneously contributed to the hardened performance of the concrete mixture by rendering it into chemically self-prestressed composite materials, thus producing SPC [58, 62, 63].

Microscopically, two distinct modes of confinement occurred to the mixtures, which were passive confinement and active confinement. Upon the slipping of a BF in a concrete block subjected to external loads, a slight dilation would be induced in the matrix surrounding the BF, which was particularly serious for the fiber with non-uniform cross-section along the length or the fiber with rough surface. Such dilations were detrimental to concrete as they may foster splitting cracks, whereas the existence of numerous fibers in the matrix, particularly the fibers in the vicinity, inhibited the crack initiation and arrest the microcracks. Such restraining actions were only developed after the BF underwent a bond slip force, thus could be described as

passive confinement [64]. In fact, a higher effectiveness of fibers at increasing fiber volumes had been reported in previous study [65], echoing this passive confinement.

On the contrary, with no BF and only EA incorporated, the confining effect could hardly be activated because the restraining action against the autogenous expansion could only be provided by steel mold. Meanwhile, particular attention shall be paid to the design of mixtures incorporating only EA because the autogenous expansion induced by EA may pose a potential threat to the quality of concrete when the addition of EA was not carefully controlled, particularly in the absence of any confinement. Thus, it is advocated that the EA should better be used in the presence of fibers. When the EA was added in the above FRC mixture, the autogenous expansion could exert compressive stresses on the BF before it was subjected to any bond slip forces due to external loads, thus providing active confinement. Subsequently, the BF would be prestressed radially inward and along the length by the autogenous expansion and restraining force against the dilation. For illustration, the muscle-inspired design of SPC is presented in Fig. 13. Utilizing the mechanism in muscle structure, the mortar became stiffer after it was transformed into SPC. To sum up, the active confinement before any bond slip forces at the initial stage and the passive confinement upon any bond slip forces at a later stage represent the primary source of the synergistic effect behind the combined use of BF and EA.

SEM images shown in Fig. 14 illustrate the fiber-matrix interface in the presence of increasing EA contents. To facilitate the comparison between different SEM images, the same scale was adopted. Apparently, a better interface was revealed when the EA content was increased from 0, 1, 2 and 3% as evidenced by the smaller gap and the smoother transitions at the interface. It is envisaged that a compression force would occur to the BF when there is an autogenous expansion induced by the EA, thus contributing to the interface by narrowing the gap in the interfacial transition zone and offering certain stress surrounding BF. The observation demonstrated that the bond of BF could be improved with the addition of EA and the effectiveness was larger at a higher EA content due to the mechanism elucidated before.

Macroscopically, the synergistic effect between BF and EA on the compressive strength and flexural strength could be up to 15.8% and 13.4%, respectively. Based on the above analysis, the synergistic effect was arising from that fact that the BF could transform the dilation and autogenous expansion into passive confinement during which the effectiveness of EA was enhanced, whilst the EA could offer the autogenous expansion by triggering the active confinement during which the effectiveness of BF was enhanced. It is worth to mention that such synergistic effect might be applicable to and more pronounced for reinforced SPC [24 ,35, 67].

6. Conclusions

This study presented a bio-inspired design of SPC by utilizing the synergistic effect between BF and EA. Considering that the sole incorporation of EA in concrete mixtures might result in a loose microstructure in the absence of confinement, BF, which has a high resistance to corrosion, could offer confinement to the concrete mixture. In this regard, a total of 16 mortar mixtures with varying BF and EA contents were developed to explore the possible synergistic effect of BF and EA in the production of SPC. Apart from the assessment of the relationship between compressive/flexural strength and fresh properties, further analysis was performed to qualitatively and quantitatively reveal the combined effect of BF and EA. Discussions on the possible mechanism behind this synergistic effect was presented from the perspective of passive and active confinement, resulting in the following conclusions:

(1) At a given EA content, the slump decreased with increasing BF content; whilst at a given BF content, the slump decreased with increasing EA content. These reductions in workability were associated with the physical effect of BF (i.e. fiber entanglement and fiber-matrix interaction) and the chemical effect of EA (i.e. hydration reaction).

(2) The individual use of BF or EA increased the compressive and flexural strengths by up to 3% and 10%, respectively. Accordingly, the simultaneous use of BF and EA enabled a higher percentage increase in strength than the sum of the percentage increases brought by their individual use. Furthermore, the strength/cement ratio increased with the BF and EA contents, leading to the highest strength/cement ratio via the combined use of BF and EA.

(3) This synergistic effect of BF and EA, reflected by the additional increase in strength due to their combined use, was up to 15.9% for compressive strength and up to 13.4% for flexural strength. The strength-workability envelops revealed that despite the negative effect of BF and EA on workability, this was compensated by the optimum concurrent flexural strength-workability performance that was observed in their combined use. Microstructural analysis demonstrated the improved interfacial transition zone in the presence of higher contents of EA at certain V_{BF}, which was in line with the macroscopic observations.

The synergistic effect was associated with the transformation of the dilation and autogenous expansion into passive confinement in the presence of BF, during which the effectiveness of EA was enhanced. Concurrently, EA facilitated autogenous expansion by triggering active confinement, during which the effectiveness of BF was enhanced. The restraining action of BF against the autogenous expansion caused by EA could trigger self-prestressing effect, leading to the development of SPC. This synergistic effect could potentially be beneficial for other performance attributes, such as the rebar-SPC bond strength, tensile strength, shear strength, torsional strength, crack resistance, blast and impact resistance, which will be assessed in upcoming

work. Further research should jointly focus on the controlled expansion process (e.g. formation of ettringite) in the presence of fibers from a chemical point of view, the development of sustainable high-performance SPC from a materials point of view and the establishment of micromechanical models from a mechanical point of view.

Acknowledgement

The authors would like to express thanks to the Department of Civil Engineering, The University of Hong Kong for offering necessary assistance and support.

Credit Author Statement

S.H. Chu: Conceptualization, Methodology, Formal analysis, Writing - Original Draft.
M. Khan: Investigation
X.W. Deng: Writing - Review & Editing
C. Unluer: Formal analysis, Writing - Review & Editing

Conflict of Interest

The authors declare that there is no known conflict of interest.

References

[1] P.N. Balaguru, S.P. Shah. Fiber-reinforced cement composites, 1992, New York, U.S.A.
[2] V.C. Li, On engineered cementitious composites (ECC), J. Adv. Concr. Tech. 1(3) (2003) 215-230.
[3] D.Y. Yoo, N. Banthia, Impact resistance of fiber-reinforced concrete–A review, Cem. Concr. Compos. 104 (2019)103389.
[4] E. Güneyisi, M. Gesoğlu, S. İpek, Effect of steel fiber addition and aspect ratio on compressive strength of cold-bonded fly ash lightweight aggregate concretes, Constr. Build. Mater. 47 (2013) 358-365.
[5] L. Huang, Y. Chi, L. Xu, P. Chen, A. Zhang, Local bond performance of rebar embedded in steel-polypropylene hybrid fiber reinforced concrete under monotonic and cyclic loading, Constr. Build. Mater. 103 (2016) 77-92.
[6] L.G. Li, Z.P. Chen, Y. Ouyang, J. Zhu, S.H. Chu, A.K.H. Kwan, Synergistic effects of steel fibres and expansive agent on steel bar-concrete bond, Cem. Concr. Compos. 104 (2019 103380.

[7] V. Gribniak, G. Kaklauskas, A.K.H. Kwan, D. Bacinskas, D. Ulbinas, Deriving stress–strain relationships for steel fibre concrete in tension from tests of beams with ordinary reinforcement, Eng. Struct. 42 (2012) 387-395.
[8] K. Wille, S. El-Tawil, A.E. Naaman, Properties of strain hardening ultra high performance fiber reinforced concrete (UHP-FRC) under direct tensile loading, Cem. Concr. Compos. 48 (2014)53-66.
[9] S. He, J. Qiu, J. Li, E.H. Yang, Strain hardening ultra-high performance concrete (SHUHPC) incorporating CNF-coated polyethylene fibers, Cem. Concr. Res. 98 (2017) 50-60.
[10] Y. Shao, S.P. Shah, Mechanical properties of PVA fiber reinforced cement composites fabricated by extrusion processing, ACI Mater. J. 94(6) (1997) 555-564.
[11] Z. Lu, A. Hanif, C. Lu, G. Sun, Y. Cheng, Z. Li, Thermal, mechanical, and surface properties of poly (vinyl alcohol) (PVA) polymer modified cementitious composites for sustainable development, J. Appl. Polym. Sci. 135(15) (2018) 46177.
[12] J.C. Liu, K.H. Tan, Fire resistance of strain hardening cementitious composite with hybrid PVA and steel fibers, Constr. Build. Mater. 135 (2017) 600-611.
[13] A.L. Hoang, E. Fehling, Influence of steel fiber content and aspect ratio on the uniaxial tensile and compressive behavior of ultra high performance concrete, Constr. Build. Mater. 153 (2017) 790-806.
[14] V.C. Li, C. Wu, S. Wang, A. Ogawa, T. Saito, Interface tailoring for strain-hardening polyvinyl alcohol-engineered cementitious composite (PVA-ECC), ACI Mater. J. 99(5) (2002) 463-472.
[15] V.C. Li, S. Wang, C. Wu, Tensile strain-hardening behavior of polyvinyl alcohol engineered cementitious composite (PVA-ECC), ACI Mater. J. 98(6) (2001) 483-492.
[16] A.K.H. Kwan, S.H. Chu, Tensile stress-strain behaviour of steel fibre reinforced concrete measured by a new direct tension test method, Eng. Struct. 176 (2018) 324–336.
[17] S.H. Chu, L.G. Li, A.K.H. Kwan, Fibre factors governing the fresh and hardened properties of steel FRC, Constr. Build. Mater.186 (2018)1228-1238.
[18] S.H. Chu, A.K.H. Kwan. A new bond model for reinforcing bars in steel fibre reinforced concrete, Cem. Concr. Compos. (2019) 103405.
[19] K.K. Mahato, K. Dutta, B.C. Ray, Static and dynamic behavior of fibrous polymeric composite materials at different environmental conditions, J. Polym. Environ. 26(3) (2018) 1024-1050.
[20] C. Frazão, B. Díaz, J. Barros, J.A. Bogasand, F. Toptan, An experimental study on the corrosion susceptibility of Recycled Steel Fiber Reinforced Concrete, Cem. Concr. Compos. 96 (2019) 138-153.
[21] D.Y. Yoo, W. Shin, B. Chun, N. Banthia, Assessment of steel fiber corrosion in self-healed ultra-high-performance fiber-reinforced concrete and its effect on tensile performance, Cem. Concr. Res. 133 (2020) 106091.

[22] Z. Lu, A. Hanif, G. Sun, R. Liang, P. Parthasarathy, Z. Li, Highly dispersed graphene oxide electrodeposited carbon fiber reinforced cement-based materials with enhanced mechanical properties, Cem. Concr. Compos. 87 (2018) 220-228.
[23] W. Alnahhal, O. Aljidda, Flexural behavior of basalt fiber reinforced concrete beams with recycled concrete coarse aggregates, Constr. Build. Mater. 169 (2018) 165-178.
[24] H. Jamshaid, R. Mishra, A green material from rock: basalt fiber–a review, J. Text. I. 107(7) (2016) 923-937.
[25] G. Wu, X. Wang, Z. Wu, Z. Dong, G. Zhang, Durability of basalt fibers and composites in corrosive environments, J. Compos. Mater. 49(7) (2015) 873-887.
[26] M. Khan, M. Cao, M. Ali, Effect of basalt fibers on mechanical properties of calcium carbonate whisker-steel fiber reinforced concrete, Constr. Build. Mater. 192 (2018) 742-753.
[27] D. Wang, Y. Ju, H. Shen, L. Xu, Mechanical properties of high performance concrete reinforced with basalt fiber and polypropylene fiber, Constr. Build. Mater. 197 (2019) 464-473.
[28] S. Chatterji, J.W. Jeffery, The volume expansion of hardened cement paste due to the presence of “dead-burnt” CaO, Mag. Concr. Res. 18(55) (1966) 65-68.
[29] P.Y. Yan, X. Qin, The effect of expansive agent and possibility of delayed ettringite formation in shrinkage-compensating massive concrete, Cem. Concr. Res. 31(2) (2001) 335-337.
[30] J.D. Carter, M. Abdulazeez, M.A. ElGawady, K.H. Khayat, FRP confinement of SCC incorporating expansive agent and saturated lightweight sand, Constr. Build. Mater. 252(2020) 118924.
[31] ACI Committee 223, ACI 223R: Guide for the Use of Shrinkage-Compensating Concrete, American Concrete Institute, USA (2010).
[32] J. Bizzozero, C. Gosselin, K.L. Scrivener, Expansion mechanisms in calcium aluminate and sulfoaluminate systems with calcium sulfate, Cem. Concr. Res. 56 (2014) 190-202.
[33] P.K. Mehta, Mechanism of expansion associated with ettringite formation, Cem. Concr. Res. 3(1) (1973) 1-6.
[34] V.S. Ramachandran, P.J. Peter, R.F. Feldman, Mechanism of hydration of calcium oxide, Nature 201(4916) (1964) 288-289.
[35] W.L. Repette, N.P. Mailvaganam, Calcium sulfoaluminate-based expansive admixtures a review, ACI Spec. Publ. 217 (2003) 177-194.
[36] R. Sahamitmongkol, T. Kishi, Tensile behavior of restrained expansive mortar and concrete, Cem. Concr. Compos. 33(1) (2011) 131-141.
[37] V. Corinaldesi, A. Nardinocchi, J. Donnini, The influence of expansive agent on the performance of fibre reinforced cement-based composites, Constr. Build. Mater. 91 (2015) 171-179.
[38] S. Ruan, J. Liu, E.H. Yang, C. Unluer, Performance and microstructure of calcined dolomite and reactive magnesia-based concrete samples, J. Mater. Civil Eng. 29(12) (2017) 04017236.

[39] R. Sahamitmongkol, T. Kishi, Tension stiffening effect and bonding characteristics of chemically prestressed concrete under tension, Mater. Struct. 44(2) (2011) 455-474.
[40] L. Mo, M. Deng, M. Tang, A. Al-Tabbaa, MgO expansive cement and concrete in China: Past, present and future, Cem. Concr. Res. 57 (2014) 1-12.
[41] Q. Cao, J. Zhou, R. Gao, Z.J. Ma, Flexural behavior of expansive concrete beams reinforced with hybrid CFRP enclosure and steel rebars, Constr. Build. Mater. 150 (2017) 501-510.
[42] S.G. Hu, Y. Li, Research on the hydration, hardening mechanism, and microstructure of high performance expansive concrete, Cem. Concr. Res 29(7) (1999) 1013-1017.
[43] W. Sun, H. Chen, X. Luo, H. Qian, The effect of hybrid fibers and expansive agent on the shrinkage and permeability of high-performance concrete. Cem. Concr. Res. 31(4) (2001) 595-601.
[44] V. Corinaldesi, A. Nardinocchi, J. Donnini, The influence of expansive agent on the performance of fibre reinforced cement-based composites, Constr. Build. Mater. 91 (2015) 171-179.
[45] A.F. Mak, M. Zhang, E.W. Tam, Biomechanics of pressure ulcer in body tissues interacting with external forces during locomotion, Annu. Rev. Biomed. Eng. (2010) 12: 29-53.
[46] K. Liu, L. Jiang, Bio-inspired design of multiscale structures for function integration, Nano Today (2011) 6(2): 155-175.
[47] L. Horny, T. Adamek, R. Zitny, Age-related changes in longitudinal prestress in human abdominal aorta, Arch. Appl. Mech. (2013) 83(6) 875-888.
[48] E. Fischer-Friedrich, Active prestress leads to an apparent stiffening of cells through geometrical effects, Biophys. J. (2018) 114(2): 419-424.
[49] L. Wu, Y. Zhang, X. Wang, Tailoring the tensile stroke of fishing line artificial muscle through prestress: a preliminary study. International Conference on Electroactive Polymer Actuators and Devices (EAPAD) XXII, 2020, vol. 11375, pp. 113751J.
[50] GB 23439-2017: Expansive agents for concrete, National Cement Standardization Technical Committee, China (2017).
[51] L.G. Li, S.H. Chu, K.L. Zeng, J. Zhu, A.K.H. Kwan, Roles of water film thickness and fibre factors in workability of polypropylene fibre reinforced mortar, Cem. Concr. Compos. 93 (2018) 196-204
[52] S.H. Chu, A.K.H. Kwan, Co-addition of metakaolin and silica fume in mortar: effects and advantages, Constr. Build. Mater. 197 (20158) 716-724.
[53] Hong Kong SAR Government, Construction Standard CS1: 2010 Testing Concrete, Volume 1, Hong Kong, China (2017).
[54] BS EN 12390-3:2019 Testing hardened concrete - Compressive strength of test specimens. British Standards Institution, London, UK (2019).
[55] BS EN 12390-5:2019 Testing hardened concrete - Flexural strength of test specimens. British Standards Institution, London, UK (2019).

[56] L.G. Li, Z.W. Zhao, J. Zhu, A.K.H. Kwan, K.L. Zeng, Combined effects of water film thickness and polypropylene fibre length on fresh properties of mortar, Constr. Build. Mater. 174 (2018) 586-593.
[57] V. Corinaldesi, A. Nardinocchi, J. Donnini, The influence of expansive agent on the performance of fibre reinforced cement-based composites, Constr. Build. Mater. 91 (2015) 171-179.
[58] A. Wang, M. Deng, D. Sun, L. Mo, J. Wang, M. Tang, Effect of combination of steel fiber and MgO-type expansive agent on properties of concrete, J. Wuhan Univ. Technol. 26(4) (2011) 786-790.
[59] P. Carballosa, J.L. García Calvo, D. Revuelta. Influence of expansive calcium sulfoaluminate agent dosage on properties and microstructure of expansive self-compacting concretes, Cem. Concr. Compos. 107 (2020) 103464.
[60] Q. Zeng, K.F. Li, T. Fen-Chong, P. Dangla, Effect of porosity on thermal expansion coefficient of cement pastes and mortars, Constr. Build. Mater. 28(1) (2012) 468-475.
[61] S. Chatterji, J.W. Jeffery, The volume expansion of hardened cement paste due to the presence of “dead-burnt” CaO, Mag. Concr. Res. 18(55) (1966) 65-68.
[62] V. Corinaldesi, A. Nardinocchi, Mechanical characterization of Engineered Cement-based Composites prepared with hybrid fibres and expansive agent, Compos. B: Eng. 98 (2016) 389-396.
[63] S. Ruan, J. Qiu, E.H. Yang, C. Unluer, Fiber-reinforced reactive magnesia-based tensile strain-hardening composites, Cem. Concr. Compos. 89 (2018) 52-61.
[64] B. Kim, J.H. Doh, C.K. Yi, J.Y. Lee, Effects of structural fibers on bonding mechanism changes in interface between GFRP bar and concrete, Compos. B Eng. 45(1) (2013) 768–779.
[65] S.H. Chu, A.K.H. Kwan, Matrix design of self-levelling ultra-high performance FRC, Constr. Build. Mater. 228 (2019) 116761.
[66] National Cancer Institute, USA.
[67] M.J. Bandelt, T.E. Frank, M.D. Lepech, S.L. Billington, Bond behavior and interface modeling of reinforced high-performance fiber-reinforced cementitious composites, Cement Concr. Compos. 83 (2017) 188–201.

List of Tables:

Table 1 Properties of the expansive agent (EA).

Properties	Value	Limit in standard
Specific surface area (m^2/kg)	420	≥ 200
Residue on 1.18 mm sieve (%)	0.2	≤ 0.5
Initial setting time (min)	150	≥ 45
Final setting time (min)	225	≤ 600
Restrained expansion in water after 7 days (%)	0.030	≥ 0.025
Restrained expansion in air after 21 days (%)	-0.005	≥ -0.020
7-day compressive strength (MPa)	25.5	≥ 20.0
28-day compressive strength (MPa)	44.5	≥ 40.0
MgO content (%)	2.62	≤ 5.0

Table 2 Mix proportions of the mortar mixes prepared in this study.

Mix	Cement (kg/m^3)	Water (kg/m^3)	EA (kg/m^3)	BF (kg/m^3)	QS (kg/m^3)
0.55-0-0.0	814	488	0	0	650
0.55-1-0.0	806	484	23	0	650
0.55-2-0.0	798	479	45	0	650
0.55-3-0.0	790	474	68	0	650
0.55-0-0.2	812	487	0	5	650
0.55-1-0.2	804	482	23	5	650
0.55-2-0.2	796	477	45	5	650
0.55-3-0.2	787	472	68	5	650
0.55-0-0.4	810	486	0	11	650
0.55-1-0.4	802	481	23	11	650
0.55-2-0.4	793	476	45	11	650
0.55-3-0.4	785	471	68	11	650
0.55-0-0.6	808	485	0	16	650
0.55-1-0.6	799	480	23	16	650
0.55-2-0.6	791	475	45	16	650
0.55-3-0.6	783	470	68	16	650

Table 3 Fresh properties of the mixes prepared in this study.

Mix	Slump (mm)	Flow diameter (mm)	Degree of levelling	SSI (%)
0.55-0-0.0	51.0	289	0.582	4.12
0.55-1-0.0	49.0	261	0.586	5.23
0.55-2-0.0	47.0	247	0.554	3.36
0.55-3-0.0	45.0	235	0.531	2.02
0.55-0-0.2	50.0	279	0.565	7.05
0.55-1-0.2	48.0	255	0.564	4.29
0.55-2-0.2	45.5	240	0.524	5.24
0.55-3-0.2	43.5	227	0.515	0.99
0.55-0-0.4	49.0	262	0.580	3.86
0.55-1-0.4	47.0	245	0.561	2.40
0.55-2-0.4	45.0	231	0.550	1.25
0.55-3-0.4	43.0	213	0.569	0.66
0.55-0-0.6	48.5	262	0.554	1.89
0.55-1-0.6	46.5	238	0.571	1.18
0.55-2-0.6	45.5	231	0.569	0.95
0.55-3-0.6	43.0	211	0.579	1.00

Table 4 Hardened properties of the mixes prepared in this study.

Mix	Compressive strength		Flexural strength	
	Mean (MPa)	S.D. (MPa)	Mean (MPa)	S.D. (MPa)
0.55-0-0.0	36.4	0.7	6.93	0.13
0.55-1-0.0	36.8	2.3	6.96	0.75
0.55-2-0.0	37.0	1.3	7.37	0.07
0.55-3-0.0	37.5	0.8	7.59	0.72
0.55-0-0.2	37.3	1.4	6.98	0.48
0.55-1-0.2	38.5	2.6	7.54	0.14
0.55-2-0.2	39.1	1.4	7.74	0.11
0.55-3-0.2	39.3	1.6	8.11	0.07
0.55-0-0.4	37.1	1.4	7.52	0.04
0.55-1-0.4	38.1	0.8	7.71	0.18
0.55-2-0.4	39.6	2.0	8.12	0.54
0.55-3-0.4	41.0	0.8	8.59	0.56
0.55-0-0.6	36.5	0.8	7.65	0.22
0.55-1-0.6	39.3	1.5	8.61	0.43
0.55-2-0.6	41.8	1.4	8.42	0.47
0.55-3-0.6	43.3	0.8	8.89	0.33

Table 5 Percentage increase in the compressive and flexural strengths of the mixes in comparison to the plain mix prepared in this study.

The addition of	Increase in compressive strength (%)	Increase in flexural strength (%)
0.2% BF at 0% EA	2.5	0.8
0.2% BF at 1% EA	4.6	8.3
0.2% BF at 2% EA	5.7	5.0
0.2% BF at 3% EA	4.8	6.8
0.4% BF at 0% EA	2.0	8.5
0.4% BF at 1% EA	3.4	10.8
0.4% BF at 2% EA	7.0	10.2
0.4% BF at 3% EA	9.3	13.1
0.6% BF at 0% EA	0.2	10.4
0.6% BF at 1% EA	6.9	23.6
0.6% BF at 2% EA	12.9	14.3
0.6% BF at 3% EA	15.6	17.1
1% EA at 0.0% BF	1.1	0.5
1% EA at 0.2% BF	3.1	8.0
1% EA at 0.4% BF	2.5	2.5
1% EA at 0.6% BF	7.8	12.5
2% EA at 0.0% BF	1.6	6.4
2% EA at 0.2% BF	4.8	10.9
2% EA at 0.4% BF	6.7	8.0
2% EA at 0.6% BF	14.6	10.2
3% EA at 0.0% BF	3.0	9.6
3% EA at 0.2% BF	5.3	16.2
3% EA at 0.4% BF	10.4	14.2
3% EA at 0.6% BF	18.9	16.3

Table 6 Synergistic effect of the simultaneous inclusion of BF and EA on the compressive strengths of the mixes prepared in this study.

Mix	Increase (%)	Synergistic effect (%)
0.55-1-0.2	5.8	2.3
0.55-2-0.2	7.4	3.3
0.55-3-0.2	8.0	2.4
0.55-1-0.4	4.6	1.6
0.55-2-0.4	8.8	5.2
0.55-3-0.4	12.6	7.6
0.55-1-0.6	8.0	6.9
0.55-2-0.6	14.8	13.0
0.55-3-0.6	19.1	15.9

Note: The values in the last column are determined as the percentage increase arising from the combined use of BF and EA minus that arising from the individual use of BF at equal V_{BF} minus that arising from the individual use of EA at equal content.

Table 7 Synergistic effect of the simultaneous inclusion of BF and EA on the flexural strengths of the mixes prepared in this study.

Mix	Increase (%)	Synergistic effect (%)
0.55-1-0.2	8.8	7.6
0.55-2-0.2	11.3	4.6
0.55-3-0.2	24.2	6.7
0.55-1-0.4	11.7	2.3
0.55-2-0.4	17.3	2.3
0.55-3-0.4	21.6	5.8
0.55-1-0.6	18.4	13.4
0.55-2-0.6	20.8	4.8
0.55-3-0.6	25.2	8.3

Figure Captions:

Fig. 1. Photos showing (a) BF and (b) EA.

Fig. 2. Slump measurements of mixes with different BF and EA contents.

Fig. 3. Flow diameters of mixes with different BF and EA contents.

Fig. 4. SSI of mixes with different BF and EA contents.

Fig. 5. Compressive strengths of mixes with different BF and EA contents.

Fig. 6. Compressive strength vs. cement content of mixes with different BF contents.

Fig. 7. Compressive strength/cement ratios of mixes with different BF and EA contents.

Fig. 8. Flexural strengths of mixes with different BF and EA contents.

Fig. 9. Flexural strength vs. cement content of mixes with different BF contents.

Fig. 10. Flexural strength/cement ratios of mixes with different BF and EA contents.

Fig. 11. Compressive strength versus workability.

Fig. 12. Flexural strength versus workability.

Fig. 13. Muscle-inspired design of SPC, showing: (a) muscle system [56] and (b) illustration of stress distribution in SPC.

Fig. 14. SEM images of the fiber-matrix interface for fiber reinforced mixtures containing: (a) 0% EA, (b) 1% EA, (c) 2% EA, and (d) 3% EA.

List of Figures:

(a)

(b)

Fig. 1. Photos showing (a) BF and (b) EA.

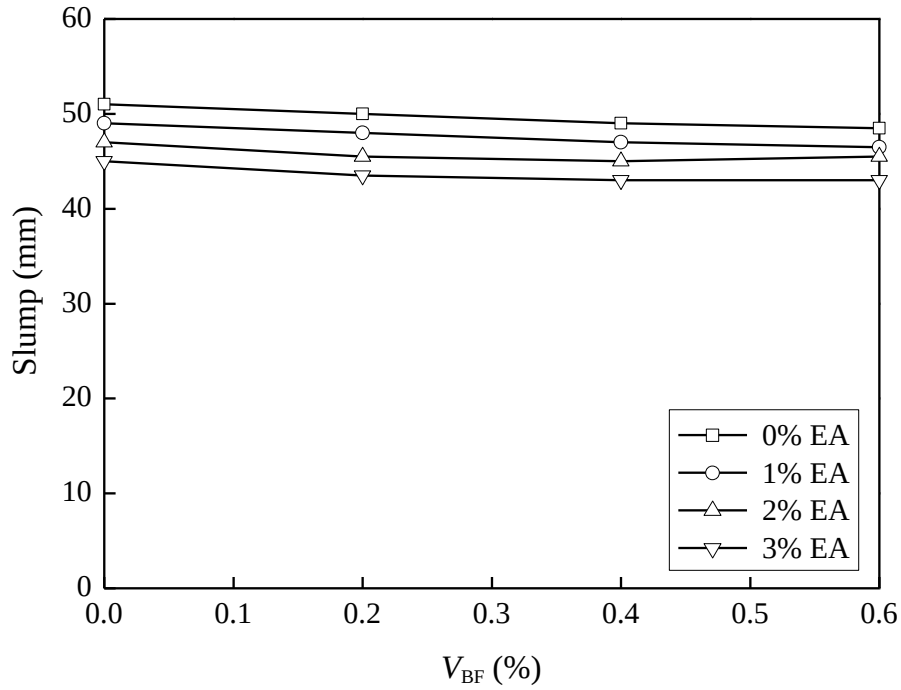

Fig. 2. Slump measurements of mixes with different BF and EA contents.

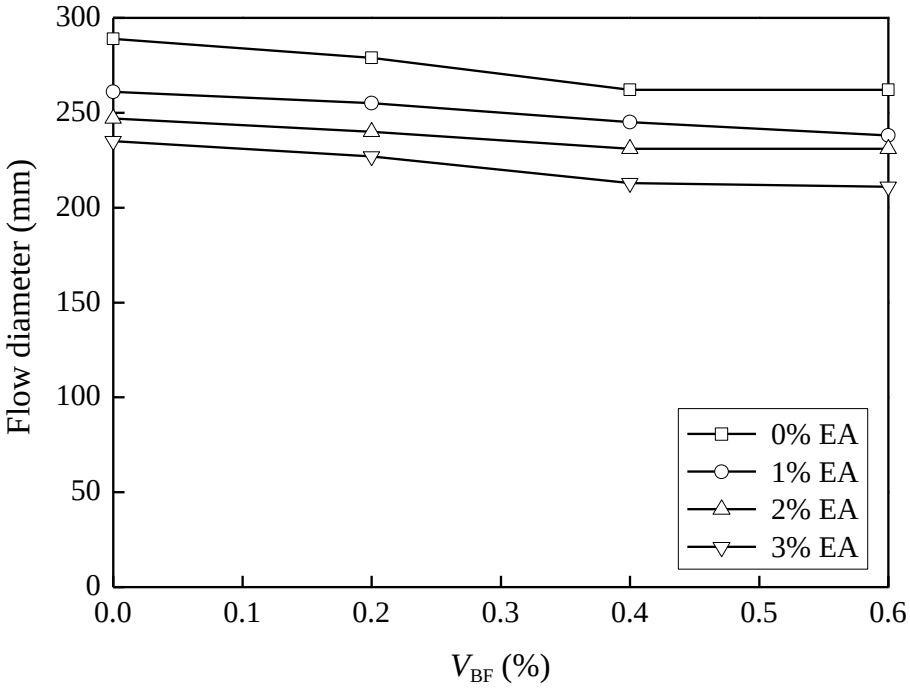

Fig. 3. Flow diameters of mixes with different BF and EA contents.

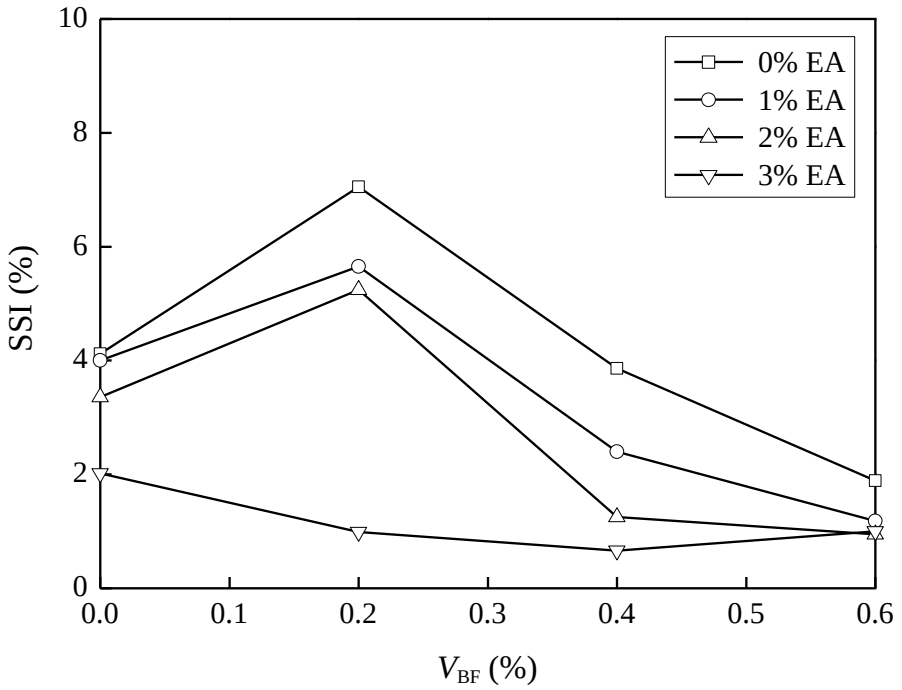

Fig. 4. SSI of mixes with different BF and EA contents.

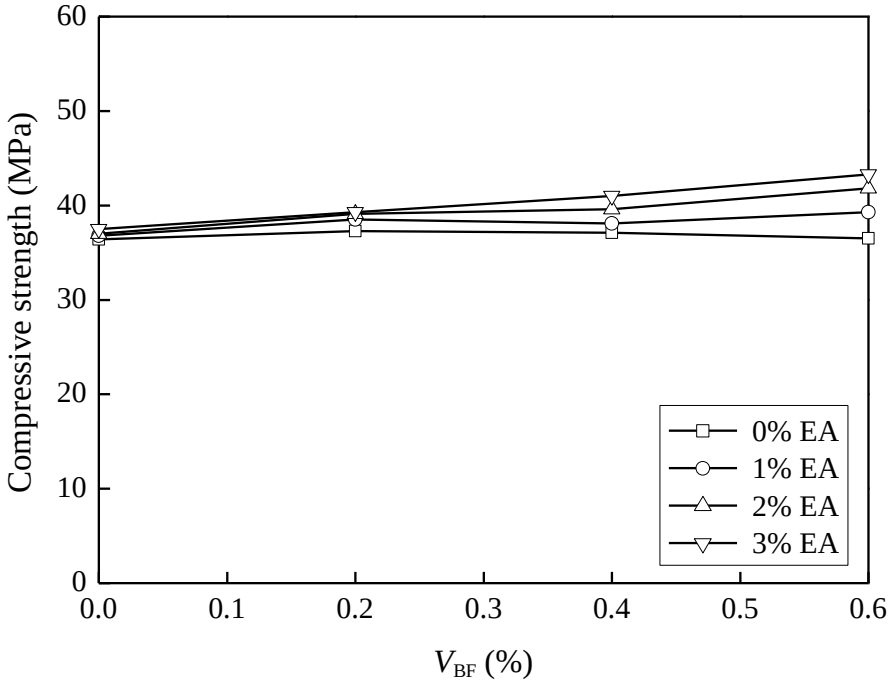

Fig. 5. Compressive strengths of mixes with different BF and EA contents.

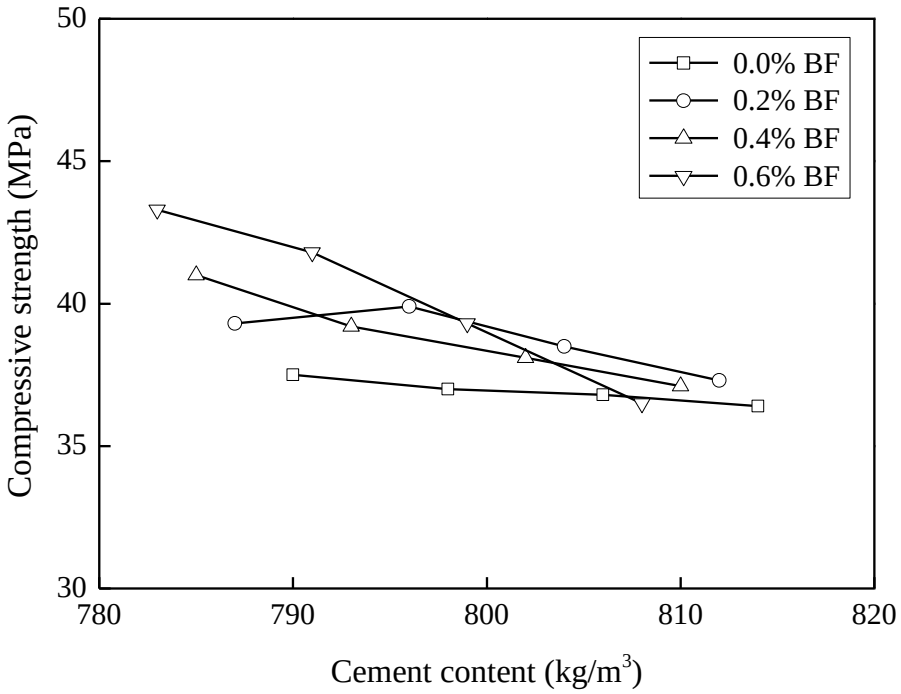

Fig. 6. Compressive strength vs. cement content of mixes with different BF contents.

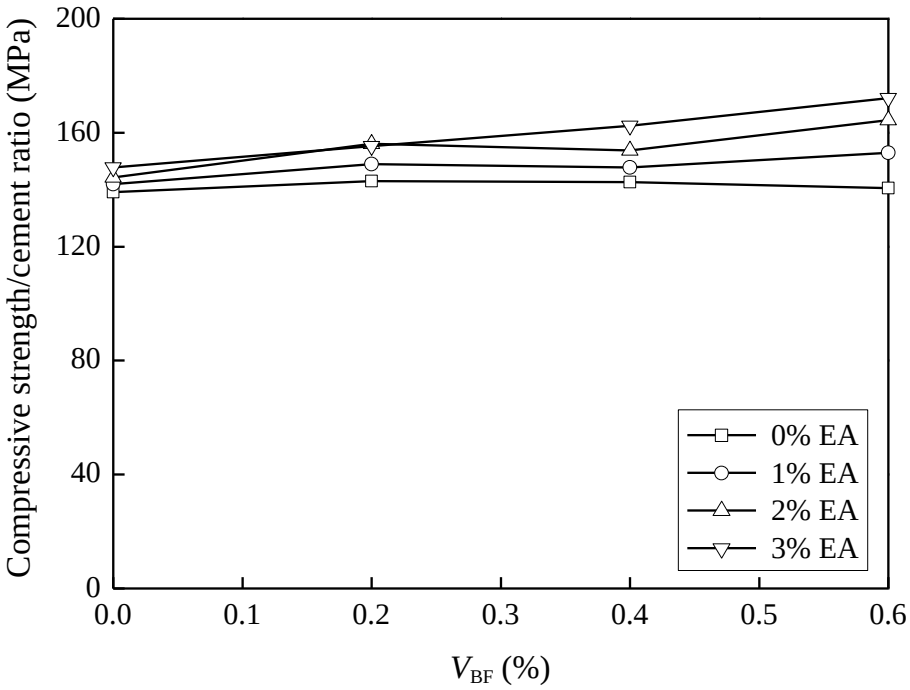

Fig. 7. Compressive strength/cement ratios of mixes with different BF and EA contents.

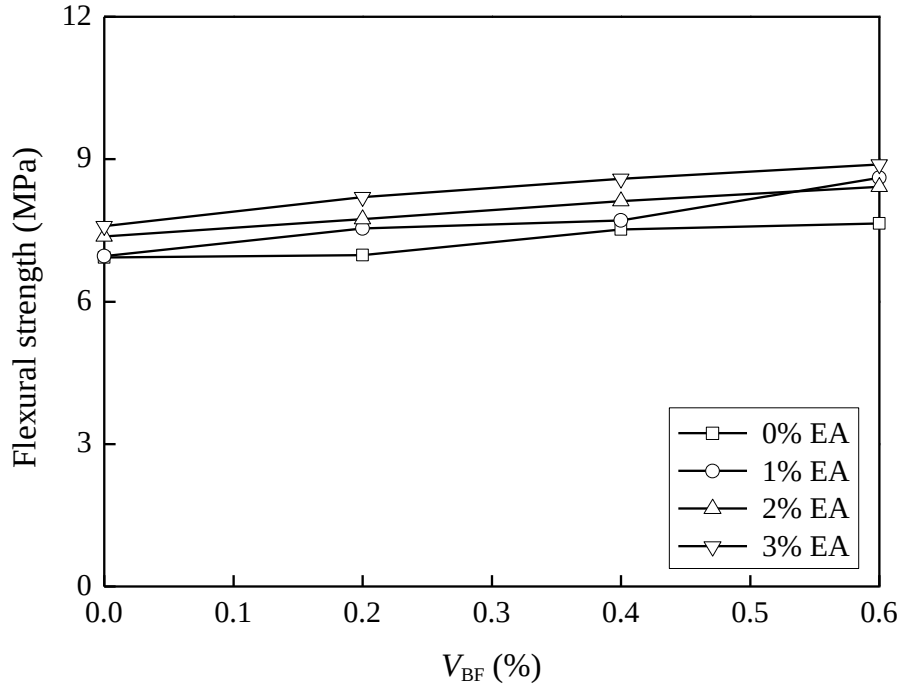

Fig. 8. Flexural strengths of mixes with different BF and EA contents.

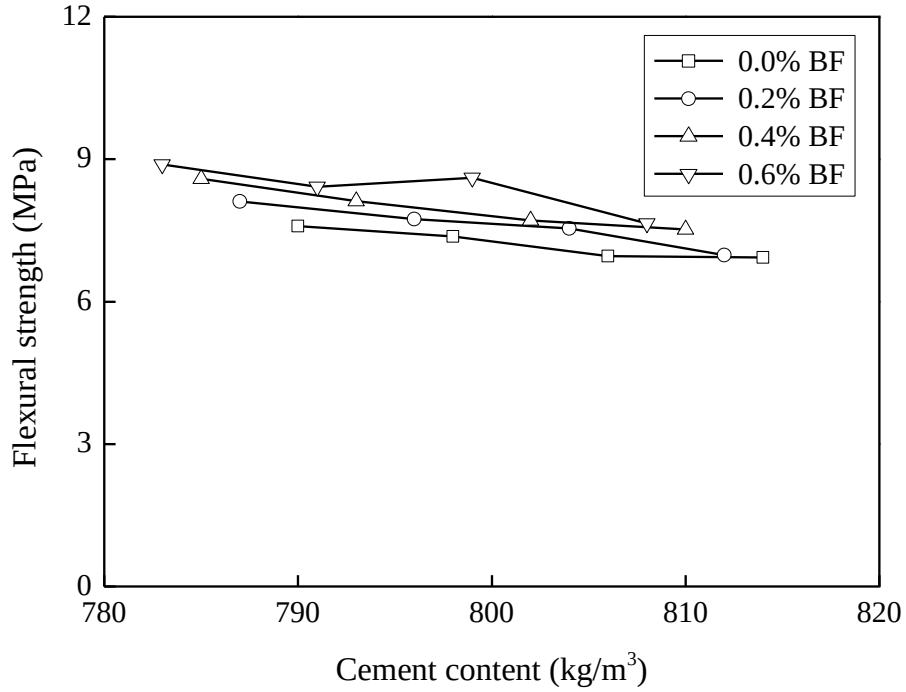

Fig. 9. Flexural strength vs. cement content of mixes with different BF contents.

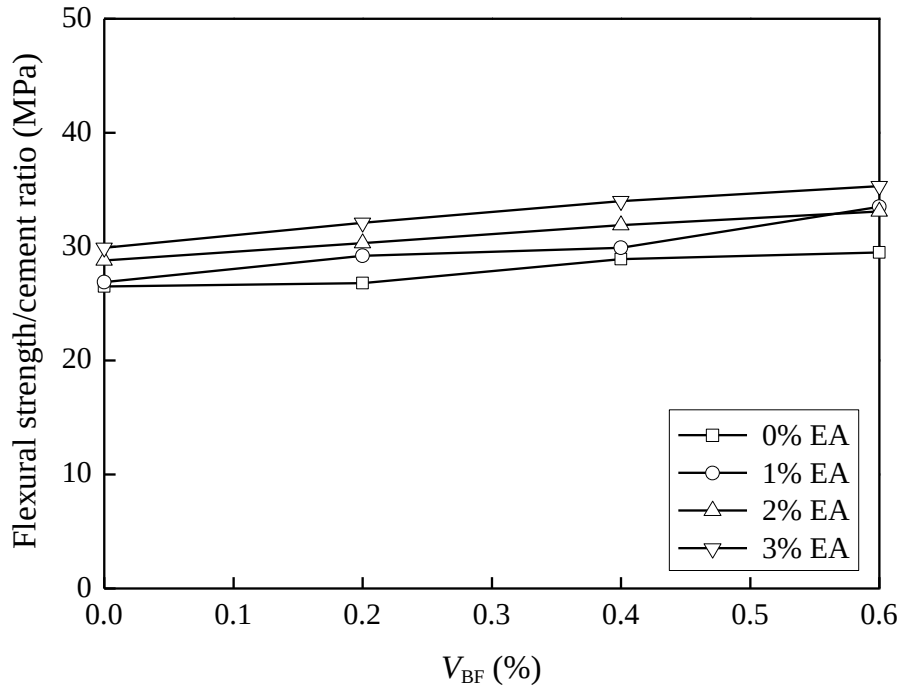

Fig. 10. Flexural strength/cement ratios of mixes with different BF and EA contents.

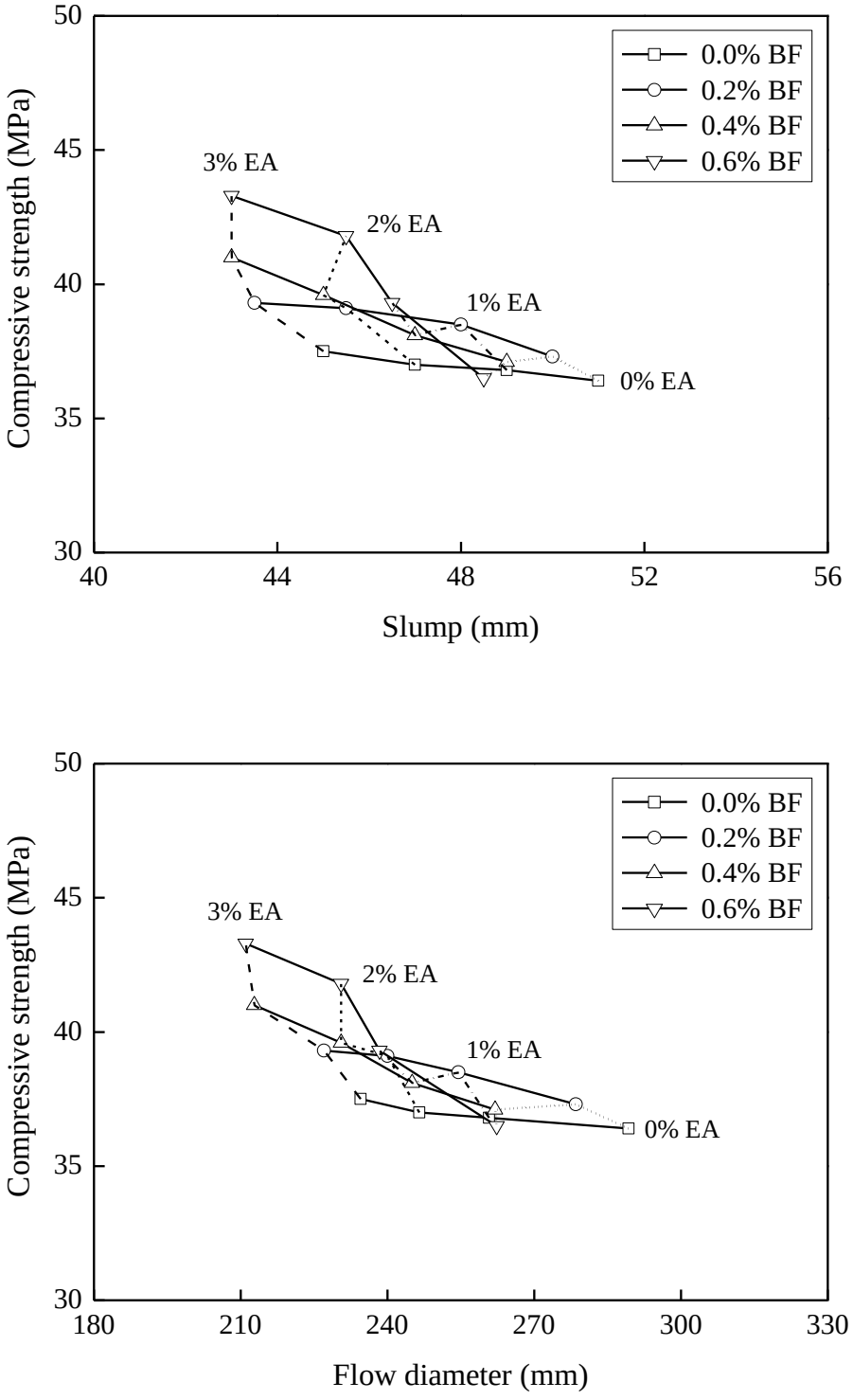

Fig. 11. Compressive strength versus workability.

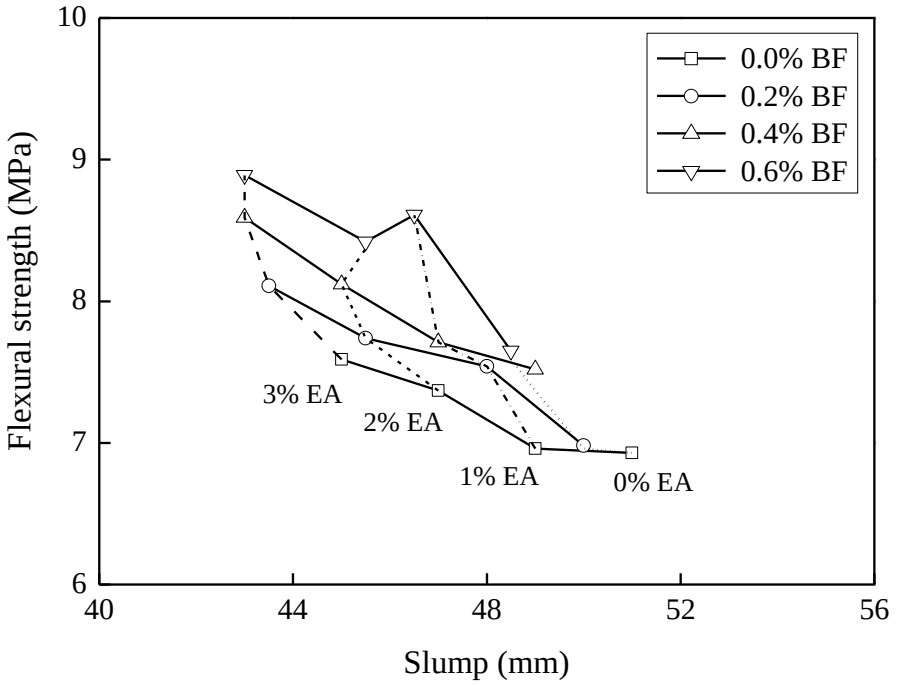

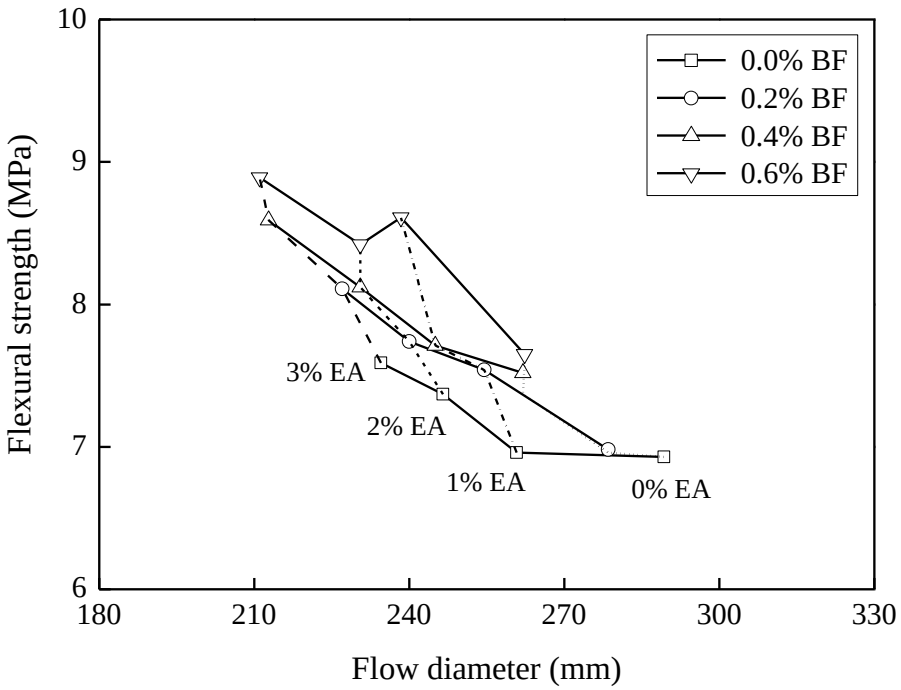

Fig. 12. Flexural strength versus workability.

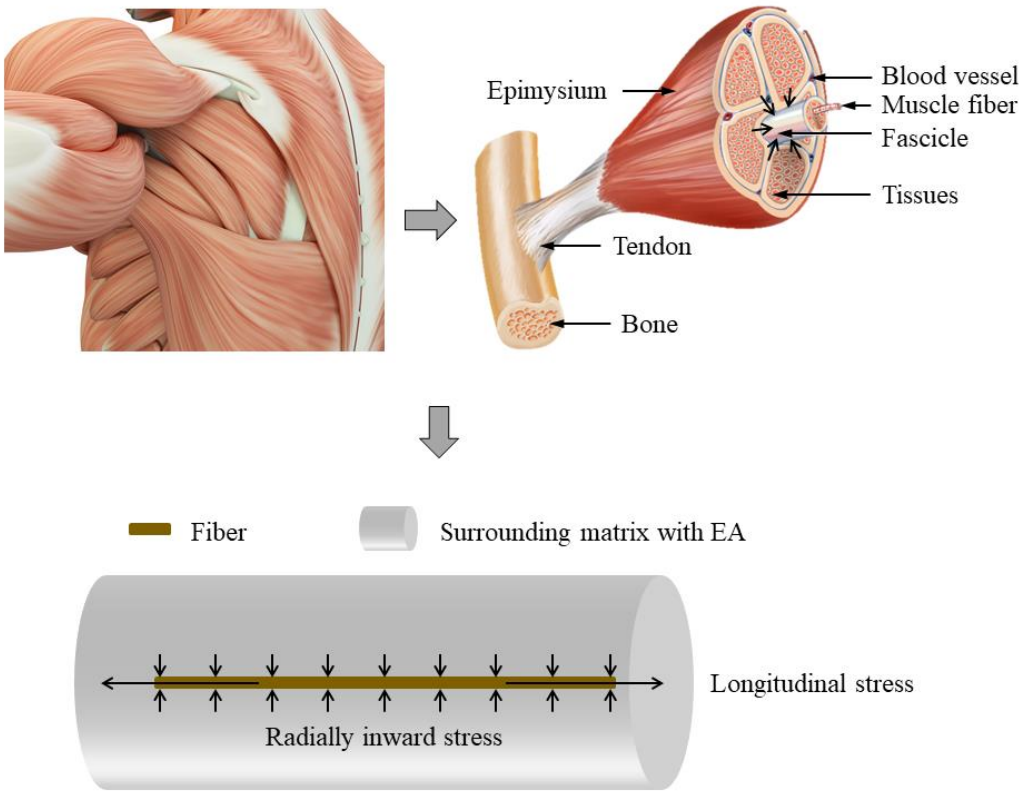

Fig. 13. Muscle-inspired design of SPC, showing: (a) muscle system [66] and (b) illustration of stress distribution in SPC.

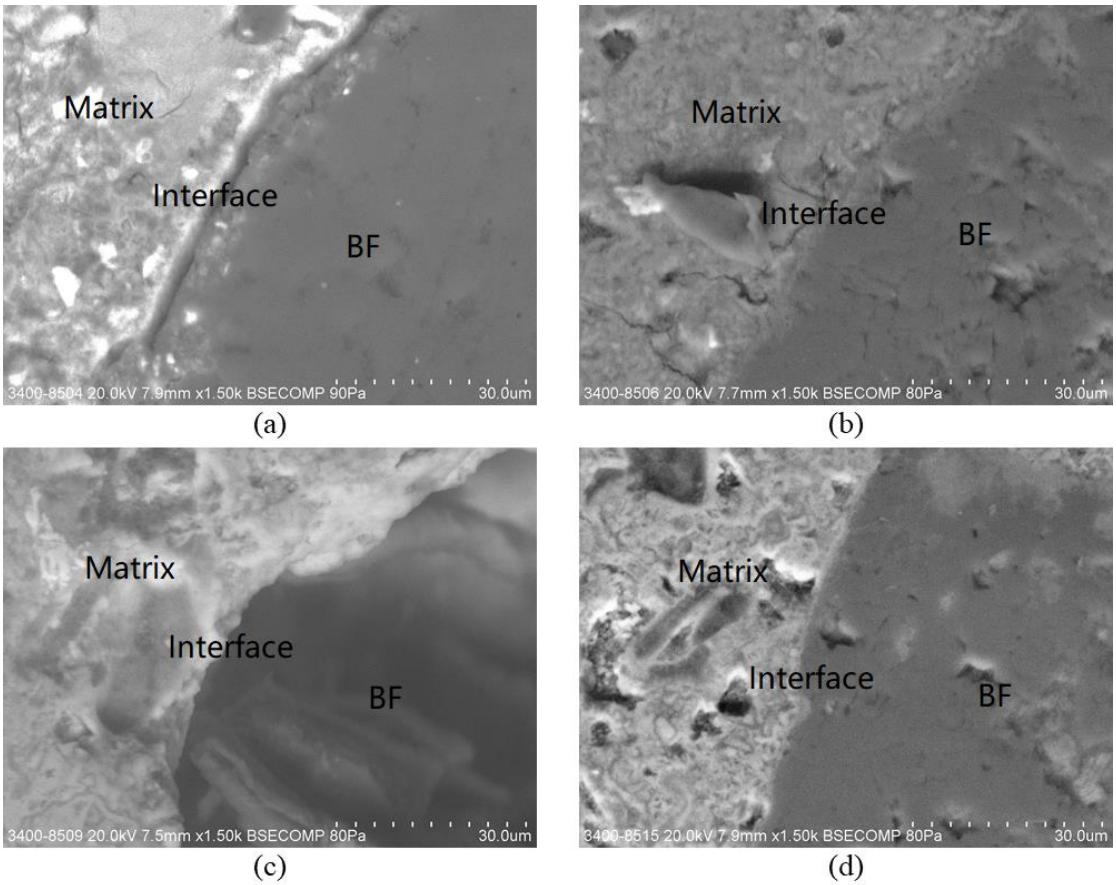

Fig. 14. SEM images of the fiber-matrix interface for fiber reinforced mixtures containing: (a) 0% EA, (b) 1% EA, (c) 2% EA, and (d) 3% EA.